X-ray absorption spectroscopy of low-molar-mass metallic complexes in pharmacy

Ioannis Nicolis,[a,b]* Emmanuel Curis,[a,b] Patrick Deschamps[c] and Simone Bénazeth[a,b]

[a]Laboratoire de Biomathématique, Faculté de Pharmacie, Université Paris V, 75006 Paris, France, [b]LURE, Université Paris XI, 91406 Orsay, France, and [c]Laboratoire de Pharmacie Galénique, Faculté de Pharmacie, Université Paris V, 75006 Paris, France. E-mail: nicolis@pharmacie.univ-paris5.fr

X-ray absorption spectroscopy provides valuable information on metallic speciation and so has a wide range of applications in bioinorganic systems. In this paper, low-molar-mass metallic complexes as used in pharmaceutical science are focused on. The results of structural studies on metal-based drugs applied as disease treatments, nutritional supplements or tools for diagnostic methods are presented. Then metal speciation (spatial and chemical distribution) in biological samples through micro-XANES imaging experiments are dealt with. Problems arising from the analysis of noisy data collected from these diluted samples are discussed.

Keywords: X-ray absorption near-edge structure (XANES); X-ray absorption spectroscopy; biological speciation; pharmaceutical science; metal-based drugs.

1. Introduction

The structure and action of drugs have to be studied nowadays at a molecular level, especially during the development of new drugs.

When biological systems contain a metal, this metal is generally an essential component of the active center. This metallic element can be the drug target (for instance, the active site of an enzyme) or can even be included in the drug molecule itself (as in the case of platinum anticancer compounds). Both the efficiency and the toxicity of the metal are dependent on the metal itself, as well as on its degree of oxidation and on its first coordination sphere. X-ray absorption spectroscopy (XAS) is a technique based on excitation of inner-shell electrons, and it gives information on the close environment of a specific element. Spectra can be recorded from complex mixtures, regardless of the physical state of the sample, including solutions and amorphous solids.

In this paper, we focus on pharmaceutical applications and we review both published research and our own results. Two kinds of applications are discussed: structural studies on metal-based drugs and metal speciation in biological samples applied to drug metabolism studies. Then we present some methodological considerations concerning the data analysis of these highly diluted samples. We conclude with perspectives concerning the XAS pharmaceutical applications at third-generation synchrotron facilities.

2. Structural studies on metal-based drugs

In this section, we focus on the local structure around organometallic compounds and trace elements, in solutions and in poorly ordered or amorphous solids.

2.1. Antitumoral organometallic compounds

2.1.1. Arsenic. Acute promyelocytic leukemia is treated by a combination of standard chemotherapy with all-*trans*-retinoic acid; nevertheless, 25% of patients have a relapse after the first treatment. For relapsing patients, a new drug is being tested, injectable solubilized arsenic trioxide, which can exist in different forms in solution, including potential degradation/oxidation products. As can be seen in Fig. 1, the As *K*-edge features are quite sensitive to the oxidation degree (edge shift) and the coordination sphere (XANES features). The spectrum recorded for the drug is very close to the arsenious acid reference solution, and the structural parameters fitted from the drug's EXAFS spectrum are identical to those of the arsenious acid. Thus, we conclude that arsenious acid is the injectable solution's main component (Nicolis *et al.*, 2001).

2.1.2. Platinum. Cisplatin is among the first antitumoral drugs to have been used, but it presents a great nephrotoxicity. Carboplatin has a similar efficiency while being much less toxic. However, in a hospital context, the stability of this compound in solutions and bags for injections is questioned, especially in the presence of chloride anions that may cause a chlorolysis of the carboplatin into cisplatin. HPLC or electrophoresis techniques have demonstrated a slow decomposition of carboplatin, but no detailed characterization of the obtained complex was proposed. By using XAS, we could observe the evolution of the platinum environment in solution. In contrast to other methods, XAS allowed us to follow the progressive transformation of carboplatin into cisplatin directly in solution, without requiring any intermediate processing. Using this method, the authors studied the pH, chloride concentration and influence on the carboplatin degradation in aqueous solution. They showed that the decomposition is too slow to be visible at neutral pH or for small chloride concentration and that light has no effect. When the pH is decreased and the chloride concentration is higher, the degradation product shows a cisplatin-type spectrum, confirming the chlorolysis (Fig. 2) (Curis *et al.*, 2000). By linear combination of cisplatin and carboplatin reference spectra, one can reproduce the time evolution of the solution composition (Fig. 3). A similar study was conducted on oxaliplatin, a third-generation platinum antitumoral drug, and led to similar conclusions (Curis *et al.*, 2001).

2.2. Metals involved in nutritional supplementation

The problem of interactions between injectable solution components also arises during artificial nutrition, either in the case of parenteral nutrition to balance surgery-injured digestive-system

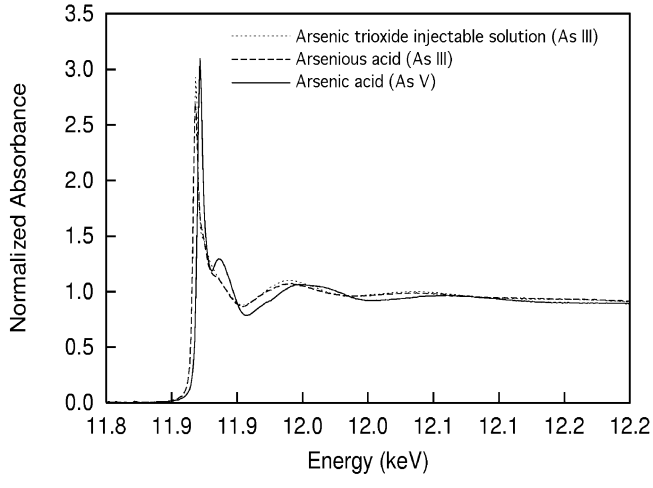

Figure 1
XANES spectra at the As *K*-edge (from Nicolis *et al.*, 2001).

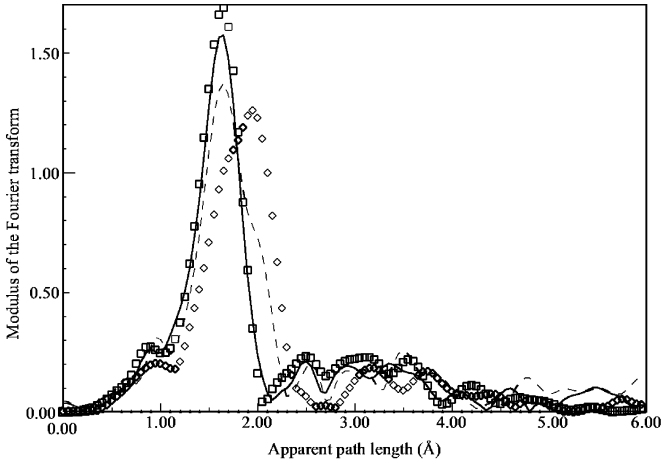

Figure 2
Evolution of the Fourier-transform modulus showing the conversion of carboplatin into cisplatin with time. Squares, solid carboplatin; solid line, carboplatin solution + HCl 0.1 *M* fourth spectrum; dashed line, carboplatin solution + HCl 0.1 *M* 21st spectrum; lozenges, solid cisplatin (from Curis *et al.*, 2000).

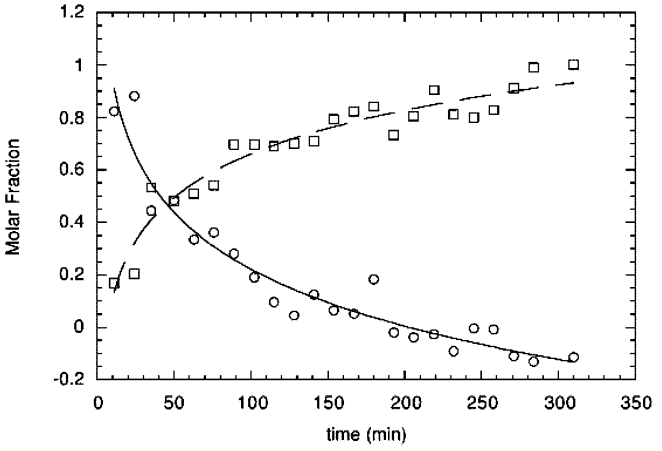

Figure 3
Evolution of the cisplatin (squares) and carboplatin (circles) fractions in solution, deduced from linear decomposition of the solution EXAFS spectrum (from Curis *et al.*, 2000).

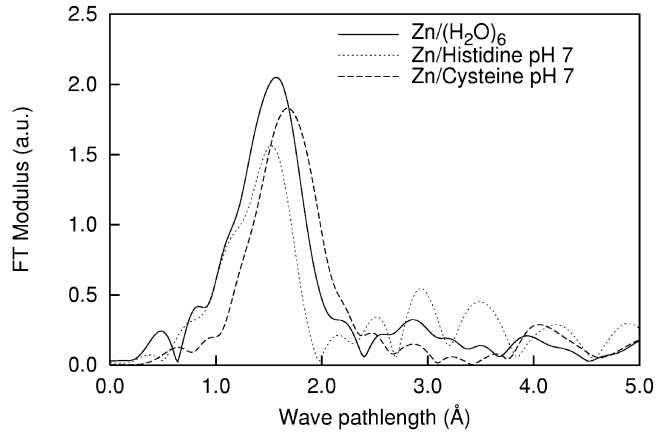

Figure 4
Fourier transforms of Zn *K*-edge EXAFS spectra, evidencing amino acid complexation (from Nicolis *et al.*, 2001).

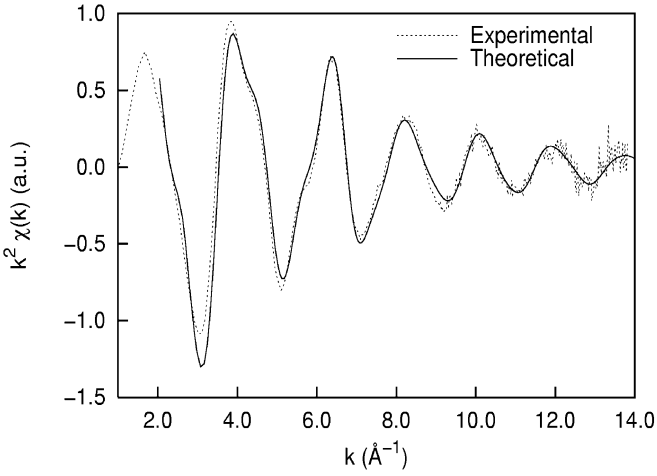

Figure 5
Fit of the EXAFS oscillations of in-solution Cu–histidine complex, using a model based on the crystalline structure of this compound (from Nicolis *et al.*, 2001).

insufficiencies or in the case of metal supplementation to correct genetic deficiencies. Practically, it is unrealistic to inject each nutriment separately, hence mixtures are prepared to limit the number of injections. However, the bioavailability of each component in these mixtures must be maintained. The main risk concerning trace elements is their complexation by amino acids, sugars or even lipids, which may limit their assimilation. Complexation can be monitored by XAS experiments to describe the local environment of the metal in solution.

2.3. Metal amino acid complexes

A first example of this type was carried out on zinc and amino acid solutions, with a complexation risk arising especially for histidine and cysteine. Reference compounds and model-solution spectra allowed the determination of the complexation pH ranges as a function of the various species concentrations. A simple comparison of the Fourier-transform (FT) experimental spectra shows that the zinc environment evolves (Fig. 4). For histidine, one observes a complexation around pH = 7. This is evidenced by the EXAFS analysis, which reveals coordination with four N atoms; for the cysteine, the EXAFS analysis shows around pH 7 the presence of two S atoms and two N atoms. These results lead to the conclusion that these complexes can be present under nutritive-solution physiological conditions, which may reduce the zinc, histidine or cysteine bioavailability. This corroborates the empirical use of a higher zinc dosage in nutritive solutions.

Menkes disease is caused by a mutation that deactivates a protein involved in copper transport, inducing a copper deficiency in humans. Therapy consists of the subcutaneous injection of a copper histidine complex, although this is not effective for severe cases or if started too late after birth. To improve the efficiency of the treatment and in a second step to develop a new oral form of the drug, the authors started a study of this complex and of other copper amino acid complexes in solid, lyophilized and aqueous solution states. Among various spectroscopies, XAS was used to characterize the copper environment. Time- and pH-dependence experiments led to a better understanding of complex formation conditions and stability. It was also shown that the complex structure in solution is close to the crystalline structure. Copper coordination involves two shells of two N atoms, with a third shell of two O atoms completing a Jahn–Teller-

effect distorted octahedron. The imidazole C atoms and three multiple-scattering paths account, respectively, for the spectrum shoulders at 4.5 $Å^{-1}$ and 5.8 $Å^{-1}$ (Fig. 5). Taking into account the conclusions of this study, a new optimized galenic form is under development (Nicolis *et al.*, 2001).

2.4. Metal carbohydrate complexes

Carbohydrates, in particular oligo- and polysaccharides, are particularly able to complex metal ions thanks to their hydroxyl residues. Hence, numerous studies have been carried out on these complexes to check their properties and, if a biological activity is recognized, to describe their structure. On the other hand, because of this complex formation, the question of a change in the metal bioavailability, as observed with amino acid complexes, is raised.

Two saccharide families are considered in relation to copper complexation. One is the 'basic' natural monosaccharide family, like fructose, glucose, galactose, xylose and ribose present in blood and in cells. The other is formed by hyaluronic acids, oligosaccharides that can be more complexing because of their carboxylate and acetamide groups. The question of metal complexation is then important, as it may lead to various applications.

Copper is known to induce metallothionein biosynthesis, hence the concentration of this protein can provide information about the copper bioavailability: the higher the metallothionein concentration, the more bioavailable the copper. To check the effect of copper complexation by saccharides, a series of complexes with the most frequent monosaccharides has been synthesized. The copper coordination sphere in these complexes was characterized by XAS: for all of them, it contains two sugar O atoms and two Cl atoms from the synthesis precursor. However, further studies demonstrated that the copper bioavailability is not altered by complexation with sugar, which is explained by the low stability of the complexes formed (Bandwar *et al.*, 1997).

Hyaluronic acids occupy a particular place from their role of signals on the cellular membrane's surface or as circulating agents, which results in a variety of structures. Moreover, they have many potential binding sites for metal ions. Some copper salts of these acids are used in ophthalmology, and it has been shown that the physical properties of these complexes are strongly dependent on the copper coordination mode, its oxidation state, the pH and the purity of the hyaluronates. XAS was successfully applied to determine the influence of synthesis conditions on the hyaluronate copper coordination (Tratar-Pic *et al.*, 2000).

Iron nutritional supplementation is a long-standing problem, especially where solubility, stability and bioavailability are concerned. Niferex, an Fe(III)/polysaccharide complex, is routinely used in therapy and has the advantage of very few side effects. Joint Mössbauer, XAS and X-ray powder diffraction studies were performed to compare the local structure and the long-distance order in this compound. Whereas the long-distance order suggests a structure close to a mineral compound, XAS shows that the local iron environment is very similar to the iron-atom site in ferritin (iron transport protein). This observation could explain the quality of this compound as an iron supplementation agent (Coe *et al.*, 1995).

In some other iron–saccharide complexes used as nutritional supplements, XAS has established the octahedral coordination of iron by saccharide O atoms, a second sphere of saccharide C atoms and, on some complexes, further Fe—Fe interactions (Rao *et al.*, 2000).

2.5. Metal-based agents for diagnostic imaging and therapeutic radiopharmaceuticals

Since heavy elements are naturally absent or rare in biological organisms, they can be easily detected even as traces in living bodies. This detection is routinely used for diagnostic purposes through their characteristic properties: sensitivity to magnetic fields, used as a contrast agent for magnetic resonance imaging (MRI); high X-ray absorption cross section, used as X-ray contrast media; radioactive disintegration, used as a radio-labeled agent for various imagery methods (gammagraphy, scintigraphy). When these products can be targeted towards a specific organ or cell, one can go further than a passive imaging agent and obtain a therapeutic effect either by sensitizing the cell to external irradiation in radiotherapy (photosensitization) or by using radioactive compounds to deliver therapeutic irradiation doses locally (therapeutic radiopharmaceuticals).

Nevertheless, the toxicity of the metal itself and of the ligands is in all cases carefully considered, and the question of the stability of the complexes and subsequently of the knowledge of the coordination shell arises.

2.5.1. MRI contrast agents. The lanthanide complexes with macrocyclic ligands such as DOTA (1,4,7,10-tetraazacyclododecane-1,4,7,10-tetraaceticacid) or DTPA (diethylenetriaminopentaacetic acid) are practically used as paramagnetic contrast agents. For some of them the applied property is their capacity to form complexes much more stable than the physiological ones. Many structural studies have been performed to explain the proton relaxivity of the complexes, but no information on solution structures was available. So, XAS studies on aqueous solutions exhibiting a pH range of 0.15–7 at different temperatures (298–363 K) have been performed. Under normal conditions, the solution structures are demonstrated to be identical to the crystalline one. From neutrality up to pH 1.5, the local environment and complex dynamics are preserved to 4.5 Å. $[Gd(DTPA)]^{2-}$ progressively dissociates from pH 0.15 to 1.5, although $[Gd(DOTA)]^{-}$ shows a slight variation from pH 1.0 to 1.5. For both complexes, only some weak temperature dependence was noted (Bénazeth *et al.*, 1998).

2.5.2. Therapeutic radiopharmaceuticals. Complexes of radioactive rhenium with the hydroxyethylidenediphosphonate (HEDP) ligand have been shown to be effective for the treatment of pain in metastatic bone cancer. During synthesis, perrhenate is reduced with stannous ions yielding a complicated mixture of species depending on reaction conditions and ligand ratio. EXAFS studies have demonstrated that monomeric or oligomeric complexes may be obtained, characterized by Re and Sn cations bridged by HEDP ligands in linear or triangular clusters with Re—Re bonds of 2.4–2.8 Å. In particular, the protocol retained for the drug synthesis seems to yield a mixture of such complexes (Elder *et al.*, 1997).

Radioiodine therapy is applied to the treatment of thyroid disorder owing to its uptake specificity by thyroid cells, which provides selective irradiation. In order to improve the dosimetry of Auger-electron-emitting ^{125}I, the molecular structure around the I atom must be known. EXAFS measurements allowed the determination of the very short range interactions of the Auger electrons in L-thyroxine and thyroglobuline (Orton *et al.*, 1996).

2.6. Metal intoxication treatment

Heavy metals are toxic to human, because they form complexes with proteins (*e.g.* mercury with sulfured proteins); lighter metals, essential as trace elements, become toxic at high concentrations. Such metal intoxication can be treated with various agents. An important class of such agents uses the chelating effect of a compound that

forms a complex that is expected to be more stable than complexes with biological compounds; it should be eliminated by the kidneys. Nevertheless, the design of these agents is challenging because of the variety of potential biological metal-fixation sites and the difficult prediction of the complex formation in biological fluids.

Transuranian metals, which are by-products of the nuclear industry, are toxic because of their chemical and radioactive properties. Neptunium is especially poisonous, and after intoxication it coexists under two oxidation states in the body: +IV and +V. A study has been made to find some chelating agents to remove neptunium. This work combines the monitoring of the neptunium elimination by classical pharmacokinetic methods and the speciation study of neptunium in the organism. Comparing the Np XANES spectra of femoral bone for mice poisoned with neptunium with reference compounds, the authors showed that the neptunium was stocked at the +IV oxidation state in the bones. Combining this result with the pharmacokinetic study, they proved the efficiency of ligands such as hydroxypyridonates in the detoxification of neptunium (Durbin *et al.*, 1998).

As is well known, selenium and mercury are highly toxic. However, when co-administrated, their toxic effects are mutually counterbalanced, which leads to the use of selenium as a mercury-poisoning antidote. This antagonism has been studied by EXAFS experiments. Se and Hg EXAFS experiments have been performed on the erythrocytes, plasma and bile of a rabbit poisoned by sodium selenite and mercury chloride. Spectra revealed the presence of a mercuric selenide core complexed with sulfur, which is thought to bind to selenoproteins in blood. The antagonistic effect is then explained by the complexation of mercury bound to selenium by this protein. The two poisons are not complexed independently to vital proteins, which could explain the detoxification activity (Gailer *et al.*, 2000).

2.7. Therapeutic metal-doped minerals

2.7.1. Ag-doped clays. Silver ions are known to be antimicrobial agents, and many attempts have been undertaken to insert silver into inorganic matrices such as zeolites or clays. Silver-doped clays for application in the treatment of burns have been envisaged, and montmorillonite was selected as it could be obtained in a well calibrated fine powder. Such a material showed a real antimicrobial activity; however, this material blackens and cannot trap regular concentrations of silver. The question of the localization of silver then arose. By applying XAS spectroscopy, it was demonstrated that silver forms triangular clusters and may coexist under metallic and ionic states in relation to the observed intrinsic instability (Keller *et al.*, 1995). After these conclusions, a new montmorillonite-based material was developed where silver is replaced by cerium. This is much more stable, and a patent about its preparation and its characterization has been registered (Castela-Papin *et al.*, 1998).

2.7.2. Zn-doped hydroxyapatite. Hydroxyapatite (HAP) is the major mineral component of bone. As such, it is used as a filling material to facilitate the reduction of bone fractures: it provides the correct mechanical resistance of bone, but it is also easily replaced by real bone tissue during the bone regeneration process. Various experiments have shown that adding small amounts of zinc (between 300 and 1000 p.p.m.) to these implants allows a faster resorption, whereas manganese in the same amounts slows down the process.

XAS, coupled with scanning electron microscopy, IR and neutron-activation analysis, allowed the composition of the Zn-doped HAP implants to be characterized more precisely. These techniques showed that the implants were polyphasic, with a major phase of crystalline HAP and other minor phases as cement between crystallites of HAP. XAS proved, by comparison with reference compounds, that zinc was mainly included in the HAP phase and not in its own phase nor in the minor phases. Its local environment includes two unusually close O atoms (about 1.79 Å) and further shells that could be interpreted either as O atoms at various distances (leading to a model of Zn replacing some Ca atoms in the unit cell) or as Ca atoms (leading to a model of a Zn atom inserted into the unit cell). The experimental results are better reproduced by the second model (Fig. 6), but this is chemically more unusual. Nevertheless, the very unusual edge feature (Fig. 7) tends to support this model (Chassot *et al.*, 2001).

This model can explain the effect of zinc in the resorption of the implant: its unusual location destabilizes the HAP cell, so it helps its degradation in the organism. During this degradation, zinc is released into the bone, which is known to activate the cicatrization processes.

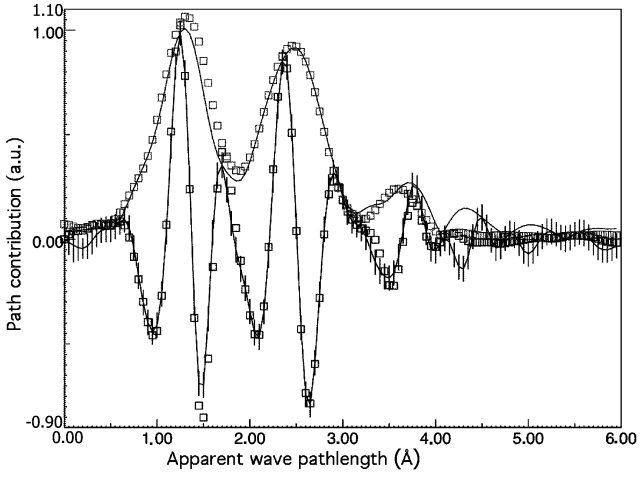

Figure 6
Comparison of experimental (lines) and model (squares) Zn-doped HAP FT, Zn *K*-edge, model with Zn inserted in the unit cell of HAP. Taking into account the error bars (drawn at 1σ), the FT is completely reproduced, since the last two small peaks are not significant (from Chassot *et al.*, 2001).

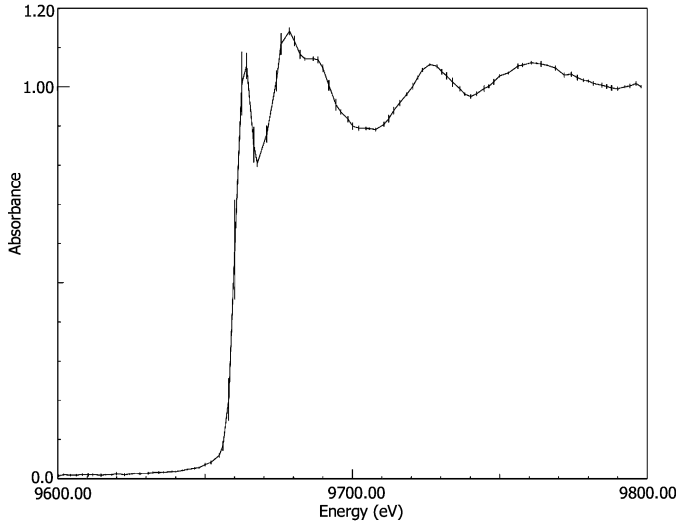

Figure 7
Zn *K*-edge of Zn-doped HAP. The unusual pre-edge intense line tends to support a linear coordination of the Zn cations. The strong features indicate a well defined Zn environment (from Chassot *et al.*, 2001).

3. Metal speciation in biological samples

In this section, we cover both endogenous and exogenous metallic components embedded in biological tissues. The aim of such speciation studies is the explanation of the therapeutic as well as the toxic properties of metals.

3.1. Macroscopic study of mineralized tissues

Because of the low brilliance of the first X-ray synchrotron sources, only quite concentrated samples could be studied until the development of third-generation sources. In a biological context, the only tissue that presents sufficient mineral element concentrations for XAS experiments is bone, thanks to its important mineralization with calcium salts. Despite the difficulty of recording Ca *K*-edge spectra, the low energy allows a better resolved XANES. Hence, the study of bone at the Ca *K*-edge was soon conducted, but the important variability of the Ca-atom sites made the analysis difficult (Harries *et al.*, 1988; Binsted *et al.*, 1982; Miller *et al.*, 1981). However, a more recent study shows that, assuming a very important dispersion in the various shells, the calcium environment can be modeled by the hydroxyapatite structure, whatever bone is considered (normal, tumoral *etc.*) and despite the variety of calcium minerals found in bone (Peters *et al.*, 2000).

A second class of concentrated biological samples includes various calcium concretions important in a medical context: they lead to the obstruction of natural (gallbladder, renal) or artificial (catheter) conduits. XAS was successfully applied to study calcium concretions formed in urinary catheters, highlighting, besides a well crystallized struvite-type phase containing magnesium, an ill crystallized apatitic phase containing the major calcium fraction (Hukins *et al.*, 1989; Cox *et al.*, 1987).

Recent studies have focused on the bone mineralization process, using models of the biological system involved in the induction of the mineral deposition in bone, cartilage and dentine. By XAS, a phosphatidyl-serine nitrogen movement was observed and assigned a key role for the deposition of the vesicle content on the preexistent mineral crystallite (Taylor *et al.*, 1998).

3.2. Spatial and chemical distribution: micro-XANES imaging

Thanks to the new generation of synchrotron radiation sources and progress in optics, it is now possible to produce microbeams and thus record the absorption spectrum of a very small part of a sample. This spectrum depends on the concentration of the element probed (fluorescence intensity) and on its local environment (edge shape and position). Thus, in a thin sample cut, one can obtain a chemical cartography of an element by performing micro-XANES, or even micro-EXAFS, experiments.

The main community using micro-XANES for heavy elements is presently in environmental science, for element speciation in soils. A bridge towards biology is emerging with the study of the evolution of these elements in plants or animals (Gardea-Torresday *et al.*, 2000; Yasoshima *et al.*, 2001). At the other end of the periodic table, endogenous light-element (C, S, P) cartography is also emerging in a biological context (Zhang *et al.*, 1996; Ade *et al.*, 1992).

As far as pharmacology is concerned, such experiments can be used to determine the localization and the chemical state of a metal in the organism. This metal can come from an accidental poisoning or from a drug delivery; it can also be a natural trace element whose behavior is followed under special conditions. Only a very few studies are currently being made in this field, and they will be presented here.

3.2.1. Control of metal toxicity. Many metals are toxic for a cell, even at a low dose. To understand the origin of this toxicity, the interaction of the metal with various cell constituents must be studied. This is a difficult task because of the various interactions between elements, the time dependence and the different metallic oxidation states. Macrophage cells are especially exposed to metal poisoning, since they represent the first defence of the organism against external invaders: exogeneous metal particles are enclosed in the foreign objects phagocyted by these cells. Hence, macrophage–metallic interaction is of great importance. To address this question, macrophage cells were cultured in a medium contaminated with metals (iron, chromium, vanadium). Then X-ray fluorescence cartography was performed and the metal oxidation degree was checked by micro-XANES spectroscopy. Results confirm the high complexity of cell metallic toxicity, showing the influence on other elements' distribution (Kitamura & Ektessabi, 2001).

Prostheses are frequently used to compensate for age- or accident-induced osseous brittleness. These metallic prostheses, however, are not always tolerated by the organism, and necrosis of the surrounding tissue can occur. To understand this mechanism and to predict the possible toxicity of the metal elements released by the prosthesis (chromium and iron for the prosthesis model considered), it is important to locate the prosthesis residues in surrounding tissues and identify the oxidation state of metals thus released. A study was therefore carried out on fine tissue cuts taken around the prostheses. X-ray fluorescence cartography and micro-XANES experiments suggest a metal grain release and their corrosion in neighboring tissues (Ektessabi *et al.*, 2001).

A recent review of applications of XANES spectroscopy to toxicology is available (Gunter *et al.*, 2002)

3.2.2. Drug monitoring. As previously stated, arsenic trioxide is used in the therapy of some leukemia types. Arsenic, after injection, circulates in the organism before being trapped in various organs, including the phaners. Arsenic localization in the hair has been investigated. From transversal cuts, insight was gained into the origin of the arsenic complexation with respect to hair's radial-structure variations. The evolution of arsenic content with time was obtained from various measurements along the hair axis. X-ray fluorescence cartography carried out on a hair cut showed that arsenic is mainly stored at the periphery of the hair (Fig. 8).

The next step of the analysis is the determination of the arsenic chemical state in the hair, which can provide information about the arsenic metabolism: for instance, is the drug trapped in the hair before or after being metabolized in its active form? To obtain this information, micro-XANES experiments were conducted on the same hair sections. Spectra were compared with a series of model

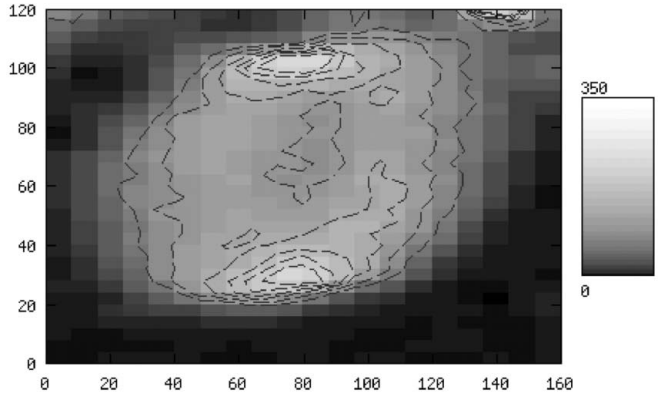

Figure 8
Cartography in a patient's hair section (scales in μm) (from Nicolis *et al.*, 2002).

compound spectra where the first coordination shell around arsenic is either sulfur or oxygen, at various degrees of oxidation (Fig. 9). Results show that, in hair, arsenic presents the oxidation degree +III, as in the injected drug, and not +V, as in the usual metabolite (cacodylic acid). One can see the strong sensitivity of the XANES to the oxidation degree: not only formal oxidation degrees are distinguished, but also, for the same oxidation degree, differences as small as the different oxidative power of carbon and oxygen are visible. This is evidenced by a comparison between the edges of arseniate $[As^{+V}O(ONa)_3]$ and cacodylate $[As^{+V}O(Me)_2ONa]$.

Moreover, X-ray fluorescence spectra recorded along a single hair to monitor the evolution of arsenic concentration evidenced fast fluctuations following the therapy protocol, thus suggesting that arsenic is not retained in the body (Nicolis *et al.*, 2002).

3.2.3. Constitutive metal. In neurodegenerative diseases like Parkinson's or Alzheimer's, the neuronal iron concentration is increased. This increase may be related to the neuron disappearance by way of a complex formation creating cytotoxic free radicals. To check this hypothesis, the oxidation degree of iron in the neuron must be studied. Neurons extracted from deceased patients' *substantia nigra* were studied by micro-XANES experiments. It was evidenced that neural death is accompanied by iron oxidation: in normal neurons, iron is in the +II state, whereas in neuromelanin complexes observed in Parkinson's disease it is +III, which is consistent with its suspected effect of free-radical production (Yoshida *et al.*, 2001).

4. Problems in the analysis of biological samples' spectra

Despite the great variety of their subjects, the studies presented in this article share a common aspect: the amount of irradiated metallic element is low, either because of the sample dilution or because of the small beam size, so collected data are noisy. However, one needs more and more precise information. To conciliate these two apparently contradictory aspects, methods must be developed to estimate the quality of the measurement and to correct systematic errors or, at least, to evaluate their effects. Giving details of the different methods proposed to deal with the different origins of noise and errors is beyond the scope of this review, and we refer the interested reader to the given references. We will just present here a short summary of some procedures accepted or proposed, to warn about these effects and the importance of checking their potential effects.

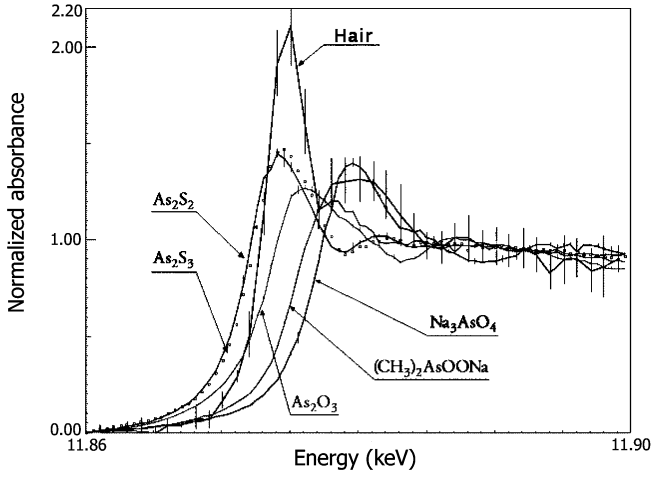

Figure 9
XANES spectra at the As *K*-edge; model compounds and patient's hair.

4.1. Statistical errors

A primary source of errors is the random noise added to the signal. This noise comes from numerous factors, many of which are difficult to control, and (because of its constant level) it is relatively more important for a small signal.

Because of the subsequent mathematical treatment applied to experimental spectra, especially for EXAFS oscillation analysis, it is better to work on a single averaged spectrum. However, that supposes, since errors are estimated when computing the average, that a method to propagate these errors through the whole analysis is available. Such a model, with only a few underlying assumptions, has been built and validated (including the step of the Fourier transform, giving an estimate of the uncertainties on this quantity) (Curis & Bénazeth, 2000).

The step of fitting a model to the experimental data gives the structural parameters and so is an essential part of the analysis. The accuracy of the obtained parameters depends, of course, on the quality of the experimental spectrum and of the model. However, this dependence varies with the fitting method and is not always obvious. Typical statistical results show that the method giving the lowest uncertainties is the maximum-likelihood method. To apply it, the experimental distribution of the errors must be known. In general, a Gaussian (normal) distribution can be assumed, in which case the maximum-likelihood method is almost equivalent to least squares (Curis & Bénazeth, 2001).

To obtain values of uncertainties of the fitted parameters, one must go further in the analysis. Most often, an analytic formula is used, but this relies on various hypotheses, including a linear model for the fitted parameters. This hypothesis is not rigorous for X-ray absorption models, so it is preferable to check it or, better, to avoid it. Monte Carlo simulations are a powerful tool for this purpose. They have been used in the past, and we are currently studying them in more depth (Ellis, 1995; Filipponi, 1995; Curis, 2001).

A completely different approach is also investigated: the use of Bayesian techniques, starting from *a priori* hypotheses and observed data, to return to the initial conditions (Krappe & Rossner, 1999, 2000; Rossner & Krappe, 2001). These techniques are still in development and are not yet used for biological samples.

4.2. Systematic errors

Noise is not the only source of errors in experimental data analysis. All models rely on various approximations, not always verified in practice. In the case of micro-XANES studies, an experimental spectrum is compared with a reference database, but the two spectra are not recorded under the same conditions. The observed differences, if weak, may then result only from different experimental conditions.

If we do not account for the theoretical model insufficiencies in EXAFS or XANES experiments, then the approximations mainly concern the sample behavior (its stability under the beam, its homogeneity) and the sample environment (stability and size of the beam, linearity of the detectors *etc.*). Although the importance of 'ideal' conditions is well known, there is not yet, to our knowledge, any protocol allowing one to quantify *a posteriori* the importance of these effects for a quasi-ideal experiment.

5. Conclusion and perspectives

The various results presented in this paper, if not exhaustive, demonstrate the extent of XAS applications in biology and, more precisely, in pharmaceutical research. However, to extract complete information from these experiments, some advances in methodology are necessary. As far as experimental limits are concerned, the increasing number of third-generation synchrotron radiation sources opens new perspectives. With their high brilliance, they support powerful analytical techniques for studying drug samples containing highly diluted metallic active centers. With such sources, it will be possible to gain insight into structure not only before administration but also in biological media during therapy. For instance, detection of metallic traces in blood and urine could be followed by a structural determination that would help the understanding of the mechanism of action and drug metabolism. We could then access the pharmacokinetic parameters.

Such a high brilliance gives us access to time-dependent studies and has potential uses in a wide range of subjects, since it allows the use of quick EXAFS on biological samples despite their high dilution. The rapidity of acquisition also has the advantage of limiting the exposure of a sample to X-rays and hence its degradation under the beam.

These sources also enable performing of micrometre-scale cartography on small-sized biological samples, either the drug target (tissues, cells) or an accumulation organ that may permit following trace amounts of a drug. In addition, the high brilliance gives a unique opportunity to complement spatial information with chemical information, which is more relevant. This speciation information is obtained through micro-XANES, a technique for which we can predict a bright future when applied to biological contexts.

We thank all colleagues who allowed the development of X-ray absorption spectroscopy applications in the field of pharmaceutical science.

References

Ade, H., Zhang, X., Cameron, S., Costello, C., Kirz, J. & Williams, S. (1992). *Science*, **258**, 972–975.
Bandwar, R. P., Rao, C. P., Giralt, M., Hidalgo, J. & Kulkarni, G. U. (1997). *J. Inorg. Biochem.* **66**, 37–44.
Bénazeth, S., Purans, J., Chalbot, M. C., Nguyen-Van-Duong, M. K., Nicolas, L., Keller, F. & Gaudemer, A. (1998). *Inorg. Chem.* **37**, 3667–3674.
Binsted, N., Hasnain, S. S. & Hukins, D. W. (1982). *Biochem. Biophys. Res. Commun.* **107**, 89–92.
Castela-Papin, N., Keller, F., Bénazeth, S. & Souleau, C. (1998). Enregistrement INPI (No. 970 1860).
Chassot, E., Oudadesse, H., Irigaray, J.-L., Curis, E., Bénazeth, S. & Nicolis, I. (2001). *J. Appl. Phys.* **90**, 6440–6446.
Coe, E. M., Bowen, L. H., Speer, J. A., Wang, Z., Sayers, D. E. & Bereman, R. (1995). *J. Inorg. Biochem.* **58**, 269–278.
Cox, A. J., Harries, J. E., Hukins, D. W., Kennedy, A. P. & Sutton, T. M. (1987). *Br. J. Urol.* **59**, 159–163.
Curis, E. (2001). Thèse de l'Université de Paris XI, France.
Curis, E. & Bénazeth, S. (2000). *J. Synchrotron Rad.* **7**, 262–266.
Curis, E. & Bénazeth, S. (2001). *J. Synchrotron Rad.* **8**, 264–266.
Curis, E., Provost, K., Bouvet, D., Nicolis, I., Crauste-Manciet, S., Brossard, D. & Bénazeth, S. (2001). *J. Synchrotron Rad.* **8**, 716–718.
Curis, E., Provost, K., Nicolis, I., Bouvet, D., Bénazeth, S., Crauste-Manciet, S., Brion, F. & Brossard, D. (2000). *New J. Chem.* **24**, 1003–1008.
Durbin, W., Kullgren, B., Xu, J., Raymond, K. N., Allen, P. G., Bucher, J. J., Edelstein, N. M. & Shuh, D. K. (1998). *Health Phys.* **75**, 34–50.
Ektessabi, A., Shikine, S., Kitamura, N., Rokkum, M. & Johansson, C. (2001). *X-ray Spectrom.* **30**, 44–48.
Elder, R. C., Yuan, J., Helmer, B., Pipes, D., Deutsch, K. & Deutsch, E. (1997). *Inorg. Chem.* **36**, 3055–3063.
Ellis, P. J. (1995). Thèse de l'Université de Sidney, Australia.
Filipponi, A. (1995). *J. Phys. Condens. Matter*, **7**, 9343–9356.
Gailer, J., George, G. N., Pickering, I. J., Madden, S., Prince, R. C., Yu, E. Y., Denton, M. B., Younis, H. S. & Aposhian, H. V. (2000). *Chem. Res. Toxicol.* **13**, 1135–1142.
Gardea-Torresday, J. L., Tiemann, K. J., Armendariz, V., Bess-Oberto, L., Chianelli, R. R., Rios, J., Parsons, J. G. & Gamez, G. (2000). *J. Hazardous Mater.* B**80**, 175–188.
Gunter, K. K., Miller, L. M., Aschner, M., Eliseev, R., Depuis, D., Gavin, C. E. & Gunter, T. E. (2002). *Neurotoxicology*, **127**, 1–20.
Harries, J. E., Hukins, D. W. & Hasnain, S. S. (1988). *Calcif. Tissue Int.* **43**, 250–253.
Hukins, D. W., Nelson, L. S., Harries, J. E., Cox, A. J. & Holt, C. (1989). *J. Inorg. Biochem.* **36**, 141–148.
Keller, F., Bénazeth, S. & Souleau, C. (1995). *Mater. Lett.* **24**, 17–21.
Kitamura, N. & Ektessabi, A. M. (2001). *J. Synchrotron Rad.* **8**, 981–983.
Krappe, H. J. & Rossner, H. H. (1999). *J. Synchrotron Rad.* **6**, 302–303.
Krappe, H. J. & Rossner, H. H. (2000). *Phys. Rev. B*, **61**, 6596–6610.
Miller, R. M., Hukins, D. W., Hasnain, S. S. & Lagarde, P. (1981). *Biochem. Biophys. Res. Commun.* **99**, 102–106.
Nicolis, I., Dacher, P., Guyon, F., Chevallier, P., Curis, E. & Bénazeth, S. (2002). *J. Trace Microprobe Tech.* In the press.
Nicolis, I., Deschamps, P., Curis, E., Corriol, O., Acar, V., Zerrouk, N., Chaumeil, J. C., Guyon, F. & Bénazeth, S. (2001). *J. Synchrotron Rad.* **8**, 984–986.
Orton, B. R., Vorsatz, D. & Macovei, D. (1996). *Acta Oncol.* **35**, 895–899.
Peters, F., Schwarz, K. & Epple, M. (2000). *Thermochim. Acta*, **361**, 131–138.
Rao, C. P., Geetha, K. M., Raghavan, S. S., Sreedhara, A., Tokunaga, K., Yamaguchi, T., Jadhav, V., Ganesh, K. N., Krishnamoorthy, T. K., Ramaiah, V. A. & Bhattacharyya, R. K. (2000). *Inorgan. Chim. Acta*, **297**, 373–382.
Rossner, H. H. & Krappe, H. J. (2001). *J. Synchrotron Rad.* **8**, 261–263.
Taylor, M. G., Simkiss, K., Simmons, J., Wu, L. N. & Wuthier, R. E. (1998). *Cell Mol. Life Sci.* **54**, 196–202.
Tratar-Pic, E., Arcon, I., Bukovec, P. & Kodre, A. (2000). *Carbohydr. Res.* **324**, 275–282.
Yasoshima, M., Matsuo, M., Kuno, A. & Takano, B. (2001). *J. Synchrotron Rad.* **8**, 969–971.
Yoshida, S., Ektessabi, A. & Fujisawa, S. (2001). *J. Synchrotron Rad.* **8**, 998–1000.
Zhang, X., Balhorn, R., Mazrimas, J. & Kirz, J. (1996). *J. Struct. Biol.* **116**, 335–344.